Study of Microfocusing Potentialities to Improve Bioparticle Separation Processes: Towards an Experimental Approach

Christine Lafforgue-Baldas, Pascale Magaud, Philippe Schmitz, Zhang Zhihao, Sandrine Geoffroy, Micheline Abbas

Study of Microfocusing Potentialities to Improve Bioparticle Separation Processes: Towards an Experimental Approach

Christine Lafforgue-Baldas[1,2,3]*, Pascale Magaud[4], Philippe Schmitz[1,2,3], Zhang Zhihao[1,2,3], Sandrine Geoffroy[4] and Micheline Abbas[5]

[1]*Université de Toulouse, INSA, UPS, INP; LISBP, 135 Avenue de Rangueil, F-31077, Toulouse, France*
[2]*INRA, UMR792 Ingénierie des Systèmes Biologiques et des Procédés, F-31400, Toulouse, France*
[3]*CNRS, UMR5504, F-31400, Toulouse, France*
[4]*Institut Clément Ader, INSA, 135 Avenue de Rangueil, F-31077, Toulouse, France*
[5]*Laboratoire de Génie Chimique, UMR 5503, BP 84234, Campus INP-ENSIACET, 4 allée Emile Monso, 31432, Toulouse cedex 4, France*

This work concerns the separation of a mixture of bi-dispersed spherical micro-particles by lateral migration at moderate Reynolds numbers. The expected differential focalization on annular rings of particles flowing in a circular micro-channel according to their size could be of interest for separation processes of poly-dispersed bio-particles suspensions. We propose an original and simple experimental method to study fluorescent particle migration at the microscale which is based on an indirect visualization of their position in a micro-channel. The particles are harvested on a plane filtration membrane put perpendicularly at the outlet of the channel. Their distribution on the membrane is then observed by fluorescent microscopy. A numerical simulation (COMSOL Multiphysics®) was developed to study the influence of membrane permeability and channel/membrane relative positions on the flow streamlines and on the subsequent size of the annular ring formed on the membrane by the focused particles. First experiments have been performed with suspensions of 1 and 4.8 μm diameter particles in order to correlate their positions to experimental conditions.

Keywords: particle migration, focusing, microfiltration, fluorescence, microscopy

1. Introduction

The context of this work is the study of lateral migration in the case of a bi-dispersed biological particle suspension flowing in a straight circular micro-channel. Its long time goal is to integrate a preliminary step of particle focusing in a microfiltration separation device to better control the fouling of the filtration membrane. Microfiltration is widely used for particles, biological cells or microorganisms removal (pharmaceutical industries, food processing, biomedical analysis...). The performance of this process is always limited by the formation of a fouling cake at the filter surface due to the accumulation of particles. In the particular case of bioparticles, the influence of particle characteristics (shape, size, surface charge...) and hydrodynamic conditions on the properties of this fouling cake, as well as the resulting filtration performances, have been already described [1–3]. Beaufort et al. [4] have performed at the local scale microfiltration of mixed microbial suspensions with different morphologies and sizes, the yeast *Saccharomyces cerevisiae* (5–7 μm) and the rod-shaped bacteria *Escherichia coli* (1–2 μm). The results have suggested that cells localization and organization inside the cake were correlated to their size and shape and affected the cake resistance. Consequently an upstream focusing of the particles depending of their size could be an original way to control particle distribution at the membrane surface and thus cake formation and the subsequent filtration performances [5].

The organization of the particles on specific equilibrium positions according to their size can be obtained directly inside the flow due to inertial effects as suggested by Poiseuille in 1838. The mechanism of the particle lateral migration for diluted suspensions has been studied by several researchers. They have proposed theoretical and experimental approaches to analyze the effect of flow and geometrical conditions (Re, particle, and channel dimensions and relative size, ...) on the equilibrium position reached by the particles and the length required to reach this position. Segré and Silberberg [6] have experimentally determined at the macroscale level, an equilibrium position on an annulus zone located at $r_{eq} = 0.62\ R$ (R: radius of the pipe) for low Reynolds number, and they have suggested that, when Re is increased, the equilibrium position is moved towards the walls. Later, Matas et al. [7] have demonstrated that the radial position of the annulus was depending on various parameters: the ratio "particle diameter/channel diameter," the Reynolds number ($r_{eq} = 0.64 \pm 0.04$ for $Re = 60$ and $r_{eq} = 0.78 \pm 0.04$ for $Re = 350$) and the particle diameter. In this work, Matas et al. have performed a direct observation of a mono dispersed 900 μm particle suspension flowing in a glass tube of 8 mm diameter (Figure 1). In this experiment, the particles were illuminated with a vertical laser beam and observed with a camera put in a lateral side of the pipe.

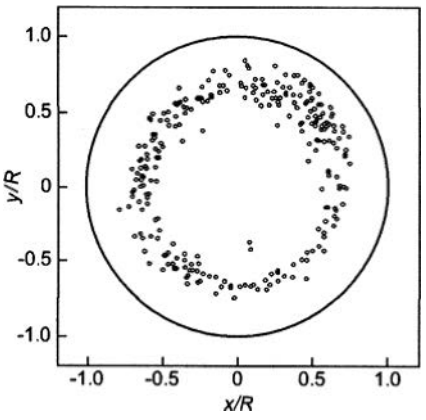

Figure 1. Experimental distribution of particles over a cross section for a Reynolds number of 60 (particle diameter of 900 μm, channel diameter of 8 mm, channel length of 2.6 m). From Matas (2004) [7]

* Author for correspondence: christine.lafforgue@insa-toulouse.fr

In other experimental studies, at the microscale, the tube section was enlarged to visualize the particle position [8], assuming that there was no deviation of the streamlines due to the enlargement. However, at the microscale, the in situ observation of the particle position remains difficult.

The aim of this work is to propose a simple method to study the focusing phenomena in the case of model micro-particles (polystyrene fluorescent microspheres) selected in the range of size of microorganisms (1 and 4.8 μm). Based on recent experimental and theoretical studies at the microscale [8–10], a very simple device has been developed. It consists of a capillary tube with outlet perpendicular to a plane microfiltration membrane. Particles flowing in the capillary tube laterally migrate and are captured by the membrane put at the outlet of the channel. Using optical fluorescence microscopy for membrane observation, it is then possible to analyze particles final positions at the membrane surface at the end of the experiment. The shape of the corresponding particle deposit which was formed is thus related to the particle spatial distribution in the outlet cross-section of the tube.

The two goals of this preliminary study are the following:

- to propose an easy and simple way to visualize the lateral migration and the focalization of the particles in micro devices,
- to determine the particle equilibrium position and the channel lengths required to reach these positions in order to analyze the effect of flow conditions and geometry of the channel on the lateral migration phenomenon.

2. Experimental Conditions

2.1. Material

2.1.1. Filtration Membranes. Different membrane materials were used in order to vary the filtration mean velocity:

- High porosity (36.7 %) and permeability (360,000 L/h·m^2/bar) silicon nitride microsieves provided from Aquamarijn® (Netherland) were plane inorganic membrane, 25 mm^2 total area, 6.3 mm^2 filtration area, with a regular arrangement of circular pores. Each microsieve consisted of 14 identical filtrating stripes with approximately 575,751 circular pores (2 μm diameter) per field. They were glued to a plastic ship.
- Low permeability ceramic membranes (from 1000 to 1500 L/h·m^2/bar) provided by TAMI industries (France) with respectively 0.2 μm and 3.5 μm mean pore size.
- Intermediate permeability acetate cellulose membrane (80,000 L/h·m^2/bar) with a mean pore size of 1.2 μm purchased from Sartorius.

2.1.2. Model Suspensions of Polystyrene Microspheres. Two types of polystyrene fluorescent microspheres 4.8 μm and 1 μm diameter density 1060 kg/m^3 have been selected to model microbial particles (Thermo Scientific, USA). They were packaged at a concentration of 1 % (w/w) in deionized water with trace amounts of surfactant and preservative to limit aggregation and promote stability. Green particles (4.8 μm) emitted fluorescence at 508 nm (excitation wavelength at 468 nm) and red particles (1 μm) emitted fluorescence at 612 nm (excitation wavelength at 542 nm). The particles were diluted in filtrated Milli-Q water in order to get a suspension concentration in a range of 8000 to 16,000 particles/mL.

2.1.3. Microscope Assays. The fluorescent particles deposited on the membrane surface were observed thanks to a LEICA FW4000 microscope equipped with specific filters corresponding to the excitation and emission wavelength of the dyed particles. The magnification of the selected objective was ×10.

2.2. Experimental Setup and Method

2.2.1. Setup. A specific experimental device was designed for this study (Figure 2). It consisted in two branches. In the first one was flowing the diluted suspension that was filled in an 8-mL stainless steel syringe (8.5 mm diameter) (Harvard Apparatus®). The syringe was pushed by a syringe pump Harvard® 1000 through a plastic tube of inner diameter equal 0.78 mm (Swagelok®). This tube was connected to a circular micro-channel in silicon nitride Polymicro Technologies® (inner diameter D = 75 μm). The microchannel was nested by a stainless steel tube to protect it. Two channel length of 5 and 60 cm were used.

The suspension flow rates were fixed according to the required Reynolds number in the channel: $\mathrm{Re} = \rho VD/\mu$, where ρ is the fluid density (kg·m^{-3}), V is the fluid velocity in the micro-channel (m/s), D is the micro-channel diameter (m), and μ is the fluid viscosity (Pa·s).

In the second branch, filtrated Milli-Q water (0.22 μm) was flowing to the filtration system. A pump (Masterflex, Bioblock Scientific, USA) and a manometer (Mano-Thermo) were used to monitor the filtration conditions (transmembrane pressure).

The distance between the membrane and the channel outlet was controlled thanks to a micrometric screw.

2.2.2. Experimental Method. The selected microfiltration membrane was mounted in the membrane holder. The whole system was then filled with water in order to surround with water the microchannel and the created jet at its outlet to avoid local perturbations due to gas/liquid interface. The stainless steel syringe was filled with the particle suspension and mounted in the syringe pump. The micro channel position (distance to the membrane) was controlled thanks to the micrometric screw. The filtration pump was run on, and its flow rate was set according to

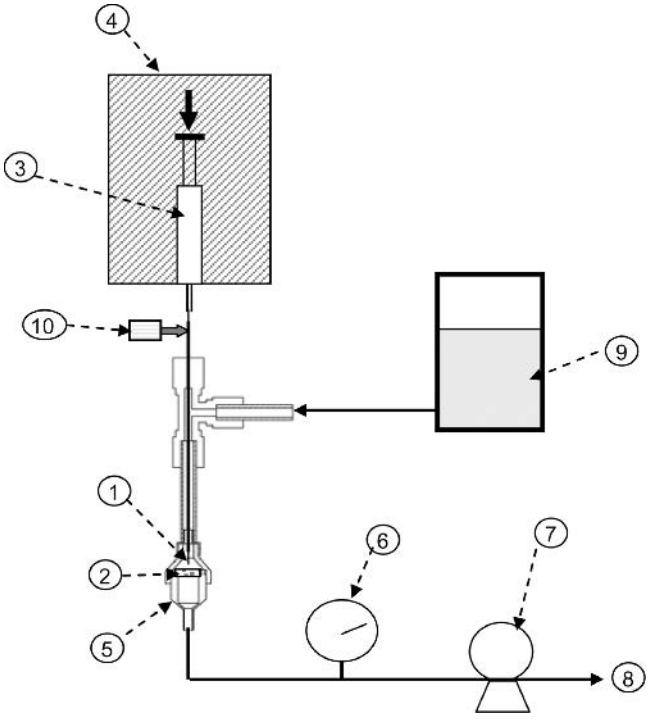

Figure 2. Experimental setup. 1: Circular micro-channel in a stainless steal tube; 2: membrane; 3: 8 mL syringe; 4: syringe pump; 5: membrane holder; 6: manometer, 7: pump; 8: liquid outlet; 9: water; 10: micrometric screw

the required filtration velocity. Pressure was controlled in order to check membrane integrity. The syringe pump was then run on at the selected flow rate, during the required time to get a sufficient number of particles deposited on the membrane. After this filtration time, the membrane was removed and observed under the microscope.

3. Theoretical Approach

3.1. Flow Model. A model based on the finite element method was developed in a previous paper by Günther et al. (2010) [11] to simulate numerically the flow in a dead-end hollow fiber module. An analog model is used to simulate the flow in the filtration chamber. For the sake of clarity, we will briefly recall the governing equations and the associated boundary conditions of the aforementioned model.

To simplify the numerical simulation, we consider an axisymmetric domain that is justified by the geometry of the filtration chamber. Therefore, the flow and the subsequent particle transport and deposition can be assumed to be axisymmetric (Figure 3). Thus, the domain consists of: (1) a cylindrical fluid region (the chamber) of height H_f and radius R_f in contact with (2) a cylindrical porous region (the membrane) of same radius R_f, height E_m, and permeability K_m (according to the given hydraulic conductivity of the membrane) and (3) a small capillary tube of length L, inner radius R_i, and outer radius R_o as depicted in Figure 3. The distance between the exit of the capillary tube and the membrane is H_0.

We consider a stationary, laminar, and incompressible flow of a Newtonian fluid in the fluid region "f." The Navier Stokes equations govern the mass and momentum balances:

$$\nabla \cdot \mathbf{u}^{\mathrm{f}} = 0 \tag{1}$$

$$\rho\left(\mathbf{u}^{\mathrm{f}} \cdot \nabla \mathbf{u}^{\mathrm{f}}\right) = -\nabla p^{\mathrm{f}} + \mu \nabla^2 \mathbf{u}^{\mathrm{f}} \tag{2}$$

where ρ is the fluid density, μ the fluid dynamic viscosity, p the pressure, and u the velocity vector. The flow in the porous domain "p" is ruled by the Darcy Brinkman equation as follows:

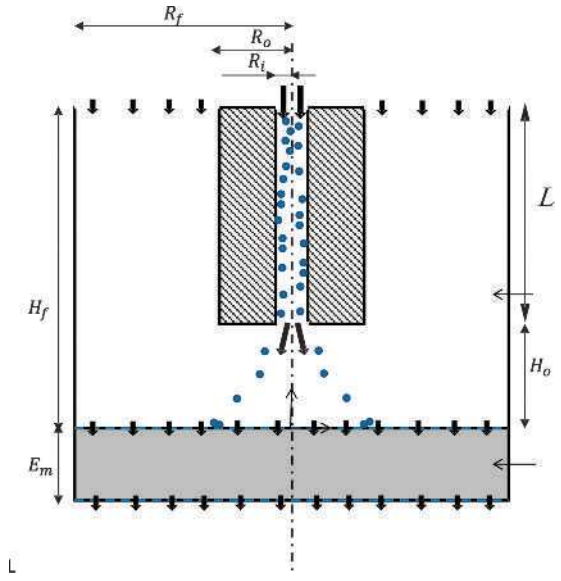

Figure 3. Scheme of the computational domain (scales not respected)

$$\nabla \cdot \mathbf{u}^{\mathrm{p}} = 0 \tag{3}$$

$$\mu_{\mathrm{eff}} \nabla^2 \mathbf{u}^{\mathrm{p}} - \nabla p^{\mathrm{p}} - \frac{\mu}{K_{\mathrm{t}}} \mathbf{u}^{\mathrm{p}} = 0 \tag{4}$$

where μ_{eff} is the effective dynamic viscosity, commonly considered as μ/ε, ε representing the porosity, and K_t is the intrinsic permeability of the porous domain. It is noted that the Darcy model is perfectly adequate to model fluid flow in porous media. However, the Darcy Brinkman model is preferred when coupling fluid and porous flow problems, in particular in the transition region where the continuity can thus be preserved for u and its derivatives.

The associated boundary conditions were chosen with respect to experimental conditions, i.e., constant working pressure in the filtration chamber, where the overall pressure difference between inlet and outlet is specified and prescribed flow rate Q at the inlet of the capillary tube. It is also assumed that there is a no slip velocity at the fluid/porous interface [12]. Finally, the whole boundary conditions with respect to r and z axis, summarized in Figure 3, can be written as:

Fluid region

$$p^{\mathrm{f}}(R_{\mathrm{o}} \le r \le R_{\mathrm{f}}, z = H_{\mathrm{f}}) = P_0 \tag{5a}$$

$$u_r^{\mathrm{f}}(0 \le z \le H_{\mathrm{f}}, r = R_{\mathrm{f}}) = 0 \tag{5b}$$

$$u_z^{\mathrm{f}}(0 \le z \le H_{\mathrm{f}}, r = R_{\mathrm{f}}) = 0 \tag{5c}$$

$$u_r^{\mathrm{f}}(H_0 \le z \le H_{\mathrm{f}}, r = R_{\mathrm{o}}) = 0 \tag{5d}$$

$$u_z^{\mathrm{f}}(H_0 \le z \le H_{\mathrm{f}}, r = R_{\mathrm{o}}) = 0 \tag{5e}$$

$$u_r^{\mathrm{f}}(z = H_0, R_{\mathrm{i}} \le r \le R_{\mathrm{o}}) = 0 \tag{5f}$$

$$u_z^{\mathrm{f}}(z = H_0, R_{\mathrm{i}} \le r \le \mathrm{R_o}) = 0 \tag{5g}$$

$$u_r^{\mathrm{f}}(z = H_{\mathrm{f}}, R_{\mathrm{i}} \le r \le R_{\mathrm{o}}) = 0 \tag{5h}$$

$$u_z^{\mathrm{f}}(z = H_{\mathrm{f}}, R_{\mathrm{i}} \le \mathrm{r} \le R_{\mathrm{o}}) = 0 \tag{5i}$$

$$u_r^{\mathrm{f}}(z = H_{\mathrm{f}}, 0 \le \mathrm{r} \le R_{\mathrm{i}}) = 0 \tag{5j}$$

$$u_z^{\mathrm{f}}(z = H_{\mathrm{f}}, 0 \le r \le R_{\mathrm{i}}) = -\frac{2Q}{\pi R_{\mathrm{i}}^2}\left[1 - \left(\frac{r}{R_{\mathrm{i}}}\right)^2\right] \tag{5k}$$

Porous region

$$p^{\mathrm{p}}(z = -E_{\mathrm{m}}, 0 \le r \le R_{\mathrm{f}}) = 0 \tag{6a}$$

$$u_r^{\mathrm{p}}(-E_{\mathrm{m}} \le z \le 0, r = R_{\mathrm{f}}) = 0 \tag{6b}$$

$$u_z^{\mathrm{p}}(-E_{\mathrm{m}} \le z \le 0, r = R_{\mathrm{f}}) = 0 \tag{6c}$$

Table 1. Theoretical data considered for numerical simulations

Membrane	Lp L/h·m^2/bar (theoretical data)	Q (μL/min)	P_o (bar)	H_o (μm)
Ceramic	1500	20	0.8	10
Ceramic	1500	20	0.8	50
Ceramic	1500	20	0.8	100
Microsieve	360,000	20	0.1	10
Microsieve	360,000	20	0.1	50
Microsieve	360,000	20	0.1	100

Porous/fluid interface

$$u_r^{\mathrm{p}}(z=0, 0\le x\le R_{\mathrm{f}}) = u_r^{\mathrm{f}}(z=0, 0\le x\le R_{\mathrm{f}}) \tag{7a}$$

$$u_z^{\mathrm{p}}(z=0, 0\le x\le R_{\mathrm{f}}) = u_z^{\mathrm{f}}(z=0, 0\le x\le R_{\mathrm{f}}) \tag{7b}$$

$$P^{\mathrm{p}}(z=0, 0\le x\le R_{\mathrm{f}}) = P^{\mathrm{f}}(z=0, 0\le x\le R_{\mathrm{f}}) \tag{7c}$$

where the subscripts r and z indicates the radial and longitudinal velocity components, respectively.

3.2. Particle Trajectory. During the filtration process, particles are transported by the fluid towards the membrane. Particle motion depends on several mechanisms such as convection, Brownian diffusion, gravity, and inertia [13]. Gravity effect can be neglected as particles are not rigorously non-buoyant, but their density is very close to the density of water. The relative magnitude of Brownian diffusion and inertia compared to convection can be estimated using the two following dimensionless numbers: Peclet, P_e, and Stokes, S_t, numbers expressed as:

$$P_{\mathrm{e}} = 6\pi\mu U_{\mathrm{f}} d_{\mathrm{p}}^2/kT \tag{8}$$

$$S_{\mathrm{t}} = \rho_{\mathrm{p}} U_{\mathrm{f}} d_{\mathrm{p}}^2/18\mu H_0 \tag{9}$$

where u_f is the characteristic filtration velocity; k, the Boltzmann constant; T, the temperature; and H_0, the characteristic length scale of the fluid domain outside the capillary tube. Using the typical data for the considered application gives $P_e > 10^3$ and $S_t < 10^{-5}$ and indicates that both Brownian diffusion and inertia have a negligible effect on the particles motion. Therefore, on the basis of the above estimates, it is assumed that particles follow the streamlines from the outlet of the capillary tube until they make contact with the membrane. Moreover, it is also assumed that the molecular interaction forces allow particles to adhere as soon as they make contact.

3.3. Numerical Results. The set of equations (1–6) was solved using the commercially-available finite element code COMSOL Multiphysics™. Numerical simulations were made in order to test the effect of the membrane permeability and of the position of the outlet of the capillary tube, H_0 on the size of the fluid capture tube at the membrane surface and to characterize the spatial distribution of the filtration velocity u_z at the membrane surface. The geometrical and hydrodynamic parameters tested are given in Table 1.

Tests were made with two types of membranes corresponding to a wide permeability range. It is shown in Figure 4 that a low permeability value, as it is the case for the ceramic membrane, favors an expansion of the streamlines coming from the capillary tube. Thus, it is expected that particles leaving the tube will be distributed on a circular disk over the membrane which size about 1 mm diameter.

On the opposite, a membrane of large permeability, such as the microsieve, will give a very small circular disk which is about 200 μm diameter (Figure 5).

Furthermore, it can be deduced from the radial distribution of filtration velocity at the membrane surface (Figure 6) that a significant gap between the end of the capillary tube and the membrane surface, say higher than 50 μm, is required to minimize the effect of pressure loss under the tube wall and to get a uniform distribution of filtration velocity at the mean velocity in the micro-channel of 20 μL/min.

We could then calculate analytically the radius of the circular disk on which particles leaving the capillary tube are expected to be distributed. Let us consider the fully developed

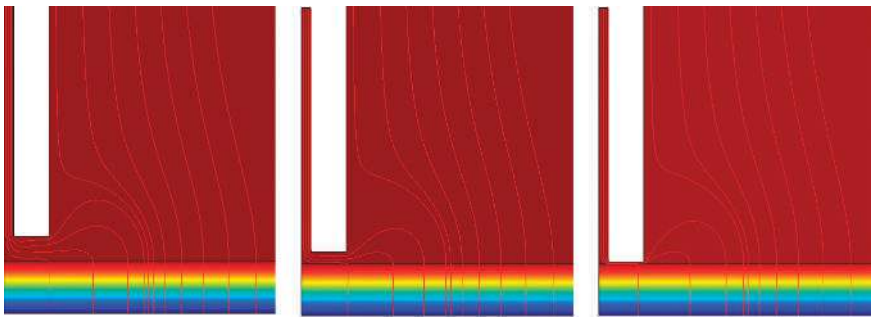

Figure 4. Pressure field and streamlines for a ceramic membrane with H_0 = 100 μm, 50 μm, and 10 μm

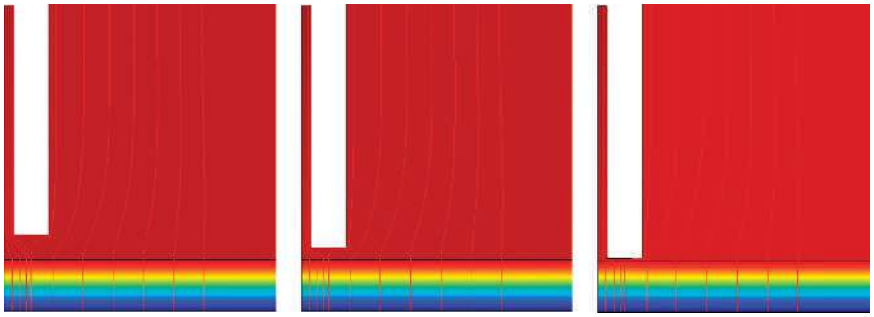

Figure 5. Pressure field and streamlines for a microsieve membrane with H_0 = 100 μm, 50 μm, and 10 μm

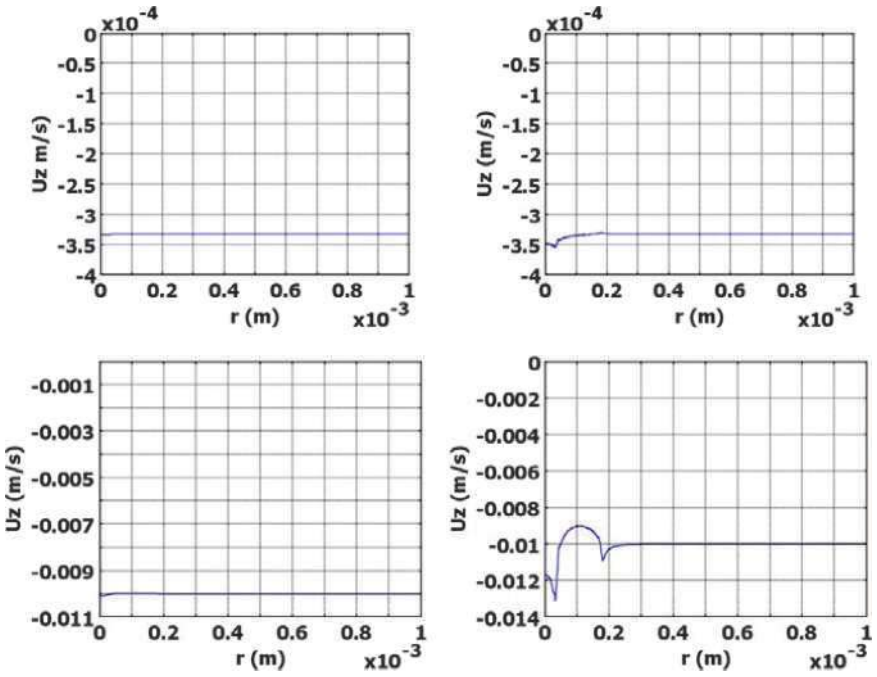

Figure 6. Radial distribution of filtration velocity for H_0 = 10 μm (right) and H_0 = 50 μm (left) for (1) a ceramic membrane (top) and (2) a microsieve membrane (bottom)

laminar flow in a circular tube of radius R_i. It is the well-known Poiseuille flow characterized by the following radial velocity profile:

$$u_z(r) = 2\frac{Q}{\pi R_i^2}\left(1-\left(\frac{r}{R_i}\right)^2\right) \quad (10)$$

Then the flow rate Q_α in the streamtube of radius αR ($0 < \alpha < 1$) can be expressed as:

$$Q_\alpha = \int_0^{\alpha R} u_z(r)\, 2\pi r\, dr \quad (11)$$

We obtain after integration:

$$Q_\alpha = 2Q\alpha^2\left(1-\frac{\alpha^2}{2}\right) \quad (12)$$

Assuming that the filtration velocity at the membrane surface is uniform, we can thus derive the expression verified by the radius of the circular disk, named R_α, crossed by the flow rate Q_α as:

$$\frac{Q_\alpha}{\pi R_\alpha^2} = L_P \Delta P \quad (13)$$

where ΔP is the transmembrane pressure which is equal to P_0 in the present problem.
Finally this can be written as:

$$R_\alpha = \alpha\sqrt{\frac{2Q\left(1-\frac{\alpha^2}{2}\right)}{\pi L_P \Delta P}} \quad (14)$$

It can be easily verified that in the particular case α = 1, we get:

$$R_1 = \alpha\sqrt{\frac{Q}{\pi L_P \Delta P}} \quad (15)$$

This is the radius of the circular disk over the membrane crossed by all the fluid leaving the tube. The corresponding values for the two membranes for a velocity in the channel of 20 μL/min are given Table 2.

4. Experimental Approach

In order to check the feasibility of this strategy to analyze particle lateral migration phenomenon in micro-channels, different experiments were performed with mono-dispersed and bi-dispersed suspensions flowing in two micro-channel lengths at various velocities.

Table 2. Calculated radius of the disk over the membrane crossed by the fluid leaving the tube

Membrane	R_1 (μm)
Ceramic	564
Microsieve	103

4.1. Influence of Channel Length. Two channel lengths of 5 and 60 cm were used; results are summarized in Table 3. From the two first observations made for the 60-cm length channel, the reproducibility of particle trajectories was checked and the concentration of the particles was adjusted. For the 60-cm length micro channel, a clear focusing of the particles was obtained. The few particles in the center of the tube were assumed to be due to the flow of some particles remaining in the channel when the membrane was taken for observation. For

Table 3. Migration of spherical 4.8 μm particle in 60 cm and 5 m cylindrical channels of 75 μm diameter

Channel length (cm)	Mean channel velocity (m/s)	Re channel	Microscopic observation
60	0.075	5.6	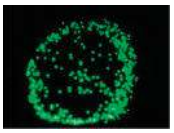
60	0.075	5.6	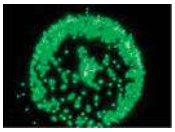
5	0.075	5.6	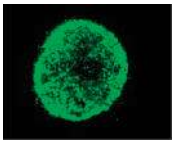

Table 4. Position of 4.8 μm and 1 μm spherical particles in a 5-cm cylindrical channel of 75 μm diameter

Channel length (cm)	Particles diameter (μm)	Mean channel velocity (m/s)	Re channel	Microscopic observation of green and red particles and composite image of the two populations
5	Polystyrene 5 μm + 1 μm	0.15	11.2	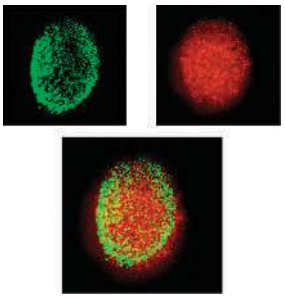
5	Polystyrene 5 μm + 1 μm	0.375	28	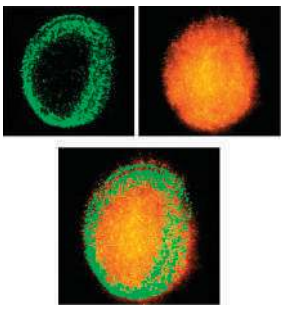

the shorter channel, the migration of the particles at their equilibrium position was not total; this observation appeared to be in agreement with Bhagat et al. (2009) and Di Carlo et al.'s (2009) [8, 14] analysis who concluded that, for a given particle diameter, the required channel length to reach equilibrium depends on the Reynolds number and the channel geometry.

4.2. Influence of Particle Diameter. Since the diameter of the spherical non deformable particle appeared to be a crucial parameter for focusing, and according to the expected application of bio-particle separation, 4.8 μm and 1 μm spherical particles were considered. The particles were mixed in the same suspension and flown in the 5 cm micro-channel for two flow rate conditions.

The image of the cross flow section at the outlet of the tube was not a perfect circle due to the deformation of the intermediate permeability selected membrane (cellulose acetate one) when transmembrane pressure was applied during filtration. However, the observation of the particle distribution on the membrane (Table 4) clearly showed the different behavior of the two populations. The distribution of the larger green particles was inhomogeneous; they were gathered on an annulus zone which seemed to be more focused for the higher Reynolds number. On the opposite, the distribution of the red smaller particles was still homogenous even for the higher Reynolds number, and they covered all the channel cross section. This qualitative observation was in agreement with the theoretical results that have demonstrated that the particle diameter has a strong effect on the length required for equilibrium establishment since the length is proportional to $(1/a_p)^3$ [8]; the smaller the particle diameter, the longer length for establishment.

Table 5. Determination of the particle equilibrium position: comparison of the measured value of the particle annulus diameter and the calculated diameter of the disk channel projection on the membrane

Mean channel velocity (m/s)	0.075	0.15
Re channel	5.6	11.2
Filtration velocity (m/s)	$0.07\ 10^{-3}$	$0.7\ 10^{-3}$
D: Analytical value of the diameter of the disk channel projection on the membrane (mm)	2.46	1.1
d: Experimental value of the particle annulus diameter (mm)	1.5 ± 0.15	0.75 ± 0.15
d/*D*	0.62 ± 0.07	0.68 ± 0.14

4.3. Towards a Quantitative Approach. In order to illustrate the particle focusing far from the channel wall, the diameter of the annulus zone of the focused green particles has been compared to the analytical value of the diameter of the channel projection calculated according to section 3.4 (Table 5).

Obviously, the accuracy of the measurements in these preliminary tests (annulus were no perfect) was low, and the results were only considered as qualitative. However, these results were consistent and in agreement with the range of values obtained by Matas et al. [7] for macroscale experiments. Optimizing the selection of the filtration membrane and better controlling the perpendicular position of the circular tube over the membrane would allow to perform future experiments exhibiting accurate measurements of the focusing position and to contribute to the study of particle lateral migration in micro-channels.

5. Conclusions

The proposed simple method to study particle migration at the microscale has appeared to be a promising tool. In this first approach, the effect of channel length and "particle to channel aspect ratio" on the lateral migration was confirmed.

According to these first experiments, the experimental device has to be improved by selecting a plane filtration membrane having an intermediate permeability but sufficiently rigid to be not modified by pressure variations. This configuration will allow accurate measurements of particle distribution and will be helpful to analyze the effect of flow conditions on lateral migration.

Further experiments with the spherical model fluorescent particles are ongoing with different objectives:

- to enlarge the range of size of the model particle (10 μm diameter particle will be used),
- to study different channels shape (circular, square, rectangle) and dimensions (diameter, length, aspect ratio)
- to determine the optimal flow conditions to obtain a differential focusing of the particle populations.

These results will allow to create a data bank in order to determine specific focusing conditions for mono or bi-dispersed particle suspensions. According to these results, new designs and improvement of separation processes could be expected.

The study could then be developed in the case of real bio-particles with fluorescent staining. In this case, the irregular shape of microorganisms would have to be considered.

Acknowledgment. The authors would like to thank Christophe Ellero for his technical support.

References

1. Mota, M.; Teixeira, J. A.; Yelshin, A. *Sep. Purif. Technol.* **2002**, *27*, 137–144.
2. Zhang, Y. P.; Fane, A. G.; Law, A. W. K. *J. Membr. Sci.* **2006**, *282*, 189–197.
3. Foley, G. *J. Membr. Sci.* **2006**, *274*, 38–46.
4. Beaufort, S.; Alfenore, S.; Lafforgue, C. *J. Membr. Sci.* **2011**, *369*, 1–2, 30–39.
5. Altena, F.; Belfort, G. *Chem. Eng. Sci.* **1984**, *39*, 343–355.
6. Segré, G.; Silberberg, A. *J. Fluid Mech.* **1962**, *4*, 136–157.
7. Matas, J. P.; Morris, J. F.; Guazzelli, E. *IFP, Institut Français du Pétrole*. **2004**, *59*, 59–70.
8. Bhagat, A. A. S.; Kuntaegowdanahalli, S. S.; Papautsky, I. *Microfluid. Nanofluid.* **2009**, *7*, 217–226.
9. Di Carlo, D.; Irimia, D.; Tompkins, R. G.; Toner, M. *Proc. Natl. Acad. Sci. U. S. A.* **2007**, *104*, 18892.
10. Magaud, P.; Geoffroy, S.; Colin, S.; Baldas, L. *2nd European Conference on Microfluidics, Toulouse*, μFLU2010, **2010**, 1–13.
11. Günther, J.; Schmitz, P.; Albasi, C.; Lafforgue, C. *J. Membr. Sci.* **2010**, *348*, 277–286.
12. Schmitz, P.; Prat, M. *AIChE J.* **1995**, *41*, 2212–2226.
13. Elimelech, M. Particle Deposition and Aggregation: Measurement, Modelling and Simulation, *Colloid and Surface Engineering Series*, **1995**, Elsevier.
14. Di Carlo D.; Edd, J. F.; Humphry, K. J.; Stone, H. A.; Toner, M. *Phys. Rev. Lett.* **2009**, *102*, 094503.